Colloid Journal, Vol. 61, No. 2, 1999, pp. 144–151. Translated from Kolloidnyi Zhurnal, Vol. 61, No. 2, 1999, pp. 164–171.

Thermodynamic Characteristics of a Small Droplet in Terms of the Density Functional Method

T. V. Bykov and A. K. Shchekin

Institute of Physics, St. Petersburg State University, ul. Ul'yanovskaya 1, Petrodvorets, St. Petersburg, 198904 Russia

Received December 25, 1997

Abstract—It was shown that, in terms of the density functional method, the self-overlapping of a surface layer in the central region of a small droplet results in a nonmonotonic dependence of the density and pressure in the droplet center on its size. The effect of this self-overlapping on the formation work of a droplet, the chemical potential of its molecule, and the surface tension in the systems with the Yukawa and Lennard-Jones potentials is described.

1. INTRODUCTION

When considering the properties of a small droplet with a strongly curved surface, it is necessary to take into account that the properties of a bulk liquid phase cannot be reached to their full extent even in the central part of a droplet. For rather small droplets (it is precisely these droplets that are of interest for the theory of homogeneous nucleation), one should take into account the effects of overlapping (in this case, self-overlapping) of surface layers. These effects may result in the nonmonotonic dependence of the density and pressure in the droplet center on its size as well as in deviations of the size dependence of droplet formation work and chemical potential of the substance comprising the droplet on the behavior predicted in terms of the capillary approximation. The self-overlapping of a droplet surface layer also may affect the dependence of the droplet surface tension on the surface curvature. It is virtually impossible to analytically describe this dependence and the dependence of the chemical potential of a molecule in a droplet confining ourselves to the Gibbs method, because the Tolman length is not yet the parameter of a theory and modifies significantly with the variation in the droplet size.

The goal of this work is to study the aforementioned effects in terms of the density functional method, which is one of the methods of the molecular theory of capillarity [1].

The problem of the determination of the thermodynamic parameters describing homogeneous nucleation in supersaturated vapors using the density functional method was treated earlier in [2–6]. Oxtoby, Evans, and Zeng [2, 3] pioneered the application of the density functional method to the problem of nucleation and obtained nonlinear integral equations for density profiles in molecular systems whose particles interact via the Yukawa [2] and Lennard-Jones potentials [3].

Hadjiagapiou [4] showed that, in the case of the Yukawa potential, the integral equation for the density profile may be reduced to a common nonlinear differential second-order equation. He also attracted attention to the density pattern in the nucleus center.

Numerical study of the dependence of droplet surface tension on the number of molecules in a droplet for various definitions of the surface tension and dividing surface was performed by Talanquer and Oxtoby [5] for systems with the Lennard-Jones potential using the generalized method of the density functional for the canonic ensemble. The role of droplet surface curvature and the compressibility of a substance comprising the droplet also was analyzed recently by McGraw and Laaksonen [6, 7] within the framework of the common density functional method.

However, a few problems still remain unresolved. Among these problems are the study of the dependences of droplet formation work and chemical potential of the molecule on droplet size, the correlation between the behavior of density and pressure in the droplet center, and the surface tension for different models of intermolecular interaction. These problems will be treated in this work. For completeness, the results will be presented for two models of intermolecular interaction potentials, namely, the Yukawa and Lennard-Jones potentials.

2. FUNDAMENTALS OF THE DENSITY FUNCTIONAL METHOD

Fundamentals of the density functional method as applied to inhomogeneous equilibrium systems have been reviewed by Evans [8]. This method has been developed further by Oxtoby and his colleagues [2, 3] as applied to problems of the theory of nucleation. We will employ the form of the density functional method reported in these works.

Let us consider the liquid–vapor system. The method is based on the idea that in order to describe the system, it is enough to be aware of its density profile

1061-933X/99/6102-0144$22.00 © 1999 МАИК "Наука/Interperiodica"

$\rho(\mathbf{r})$, i.e., the dependence of the number of particles per unit volume on their positions in space. It is assumed that the grand thermodynamic potential of such a system is a functional of this density profile. Let us denote the grand thermodynamic potential of a system by $\Omega[\rho(\mathbf{r})]$.

For an open system, the equilibrium density profile provides the extremum of the $\Omega[\rho(\mathbf{r})]$ functional. In the local approximation based on the contribution of short-range forces of repulsion and in the approximation of random phases, the grand thermodynamic potential as a functional of $\rho(\mathbf{r})$ may be written in the following form [2, 3, 8]

$$\Omega[\rho(\mathbf{r})] = \int_V d\mathbf{r} f_h[\rho(\mathbf{r})] + \frac{1}{2}\int_V\int d\mathbf{r}d\mathbf{r}' w(|\mathbf{r}-\mathbf{r}'|)\rho(\mathbf{r})\rho(\mathbf{r}') - \mu\int_V d\mathbf{r}\rho(\mathbf{r}). \quad (2.1)$$

Here, $f_h(\rho)$ is the free energy density of a system of hard spheres, $w(|\mathbf{r}-\mathbf{r}'|)$ is the contribution of two-particle interaction to the potential related to the particle attraction, μ is the chemical potential of the system under study, and V is the system volume. Representing $f_h(\rho)$ as $f_h(\rho) = \rho\mu_h(\rho) - p_h(\rho)$, where μ_h is the chemical potential and p_h is the pressure of a system of hard spheres at the given temperature T and density $\rho(\mathbf{r})$, for $\mu_h(\rho)$ and $p_h(\rho)$ we use the Carnahan–Starling formula [9]

$$\mu_h(\rho) = k_B T[\ln\eta + (8\eta - 9\eta^2 + 3\eta^3)/(1-\eta)^3],$$
$$p_h(\rho) = k_B T\rho(1+\eta+\eta^2+\eta^3)/(1-\eta)^3, \quad (2.2)$$

where k_B is the Boltzmann constant, $\eta = \pi d^3\rho/6$ is the dimensionless density, and d is the diameter of a hard sphere.

The condition of extremality $\Omega[\rho(\mathbf{r})]$ under equilibrium results in the integral equation for the equilibrium profile $\rho(\mathbf{r})$

$$\mu_h(\rho(\mathbf{r})) + \int_V d\mathbf{r}' w(|\mathbf{r}-\mathbf{r}'|)\rho(\mathbf{r}') = \mu. \quad (2.3)$$

Below, it is more convenient to use the dimensionless variables radius vector $\mathbf{u} = \mathbf{r}/d$, density η, pressure $p^* = (\pi/6)pd^3/k_BT$, interaction potential $w^*(u) = 6w(ud)/k_BT\pi$, chemical potentials $\mu^* = \mu/k_BT$ and $\mu_h^* = \mu_h/k_BT$, and grand thermodynamic potential $\Omega^* = \Omega/k_BT$. In the new variables, equation (2.3) acquires the from

$$\mu_h^*(\eta(\mathbf{u})) + \int_V d\mathbf{u}' w^*(|\mathbf{u}-\mathbf{u}'|)\eta(\mathbf{u}') = \mu^*. \quad (2.4)$$

For bulk phases, integral equation (2.4) is reduced to an algebraic equation. Solving such an equation, we find the critical temperature T_c and, for given temperature $T < T_c$, calculate the value of chemical potential $\mu_\infty(T)$ corresponding to the equilibrium between liquid and gaseous phases with a flat interface as well as the values of densities η_l and η_v for the liquid and gaseous phases, respectively. The determined values of μ_∞, η_l, and η_v are the reference values for the subsequent calculation of the density profile in the inhomogeneous droplet.

3. MODELS OF INTERMOLECULAR POTENTIAL AND THE CALCULATION ALGORITHM

The spherically symmetric solution of equation (2.4) describing the critical nucleus is of prime interest for the theory of homogeneous nucleation, because its formation work determines the height of an activation barrier of the nucleation. However, this solution of equation (2.4) corresponds to the maximum of the grand thermodynamic potential and, hence, is unstable, thus making its solution more complicated.

When spherical symmetry applies, $\eta(\mathbf{u}) = \eta(u)$, and equation (2.4) in spherical coordinates at $V \longrightarrow \infty$ acquires the following form

$$\mu_h^*[\eta(\mathbf{u})] = \mu^* - 2\pi\int_0^\infty du'u'^2\int_0^\pi d\theta\sin\theta w^*(|\mathbf{u}-\mathbf{u}'|)\eta(u'), \quad (3.1)$$

where

$$|\mathbf{u}-\mathbf{u}'| = (u^2 + u'^2 - 2uu'\cos\theta)^{1/2} \quad (3.2)$$

and θ is the azimuthal angle in the coordinate system whose z-axis coincides with the direction of vector $\mathbf{u}$.

The integration with respect to angle θ in equation (3.1) may be carried out analytically when the Yukawa or Lennard-Jones potentials are selected as the models for intermolecular interaction in the form proposed by Weeks, Chandler and Andersen [10]. The Yukawa potential in the dimensional variables has the form

$$w(r) = -\frac{\alpha\lambda^3}{4\pi}\frac{e^{-\lambda r}}{\lambda r}. \quad (3.3)$$

There are two parameters (α and λ) in equation (3.3), which may be determined independently. As was shown in [2], parameter λ slightly affects the properties of bulk phases, but has significant effect on the properties of the surface layer. Being more interested in qualitative than quantitative aspects of the calculations performed using the Yukawa potential, let us assume, according to [4], that $\lambda = 1/d$. The final form of equation (3.1) for the Yukawa potential with an allowance for (3.2) and (3.3) is as follows:

$$\mu_h^*[\eta(u)] = \mu^* - \frac{\alpha^*}{2u}\int_0^\infty du'u'\eta(u') \times [\exp(-|u-u'|) - \exp(-|u+u'|)]. \quad (3.4)$$

The selection of the Lennard-Jones potential in the form proposed by Weeks, Chandler, and Andersen [10],

$$w(r) = \begin{cases} -\varepsilon, & r < r_{\min}, \\ 4\varepsilon((\sigma/r)^{12} - (\sigma/r)^{6}), & r > r_{\min}, \end{cases} \quad (3.5)$$

as the model of intermolecular interaction is more substantiated from the physical point of view. In this equation, $r_{\min} = 2^{1/6}\sigma$; ε and σ are the parameters of the Lennard-Jones potential. According to [3], let us assume that $d(T) = \dfrac{a_1 T + b}{a_2 T + a_3}\sigma$ (the values of a_1, a_2, a_3, and b have been determined in [3]). Note that the piece-wise nature of function (3.5) leads [when it is substituted into (3.1)] to a very cumbersome expression, which is not reported here.

Let us consider the procedure for the solution of equation (3.1). Let us seek this solution by the iteration procedure substituting the initial approximation for $\eta(u')$ into the inegrand in (3.1). As was shown in [2, 3], such a procedure, generally speaking, does not stably converge to the solution corresponding to the critical nucleus, because this nucleus is in a state of unstable equilibrium with the vapor. Therefore, first, it is necessary to choose an adequate initial approximation, and second, to choose a criterion according to which the iteration process should be terminated at the moment when the result is most close to the desired profile density in a critical nucleus.

According to [2, 3], we use the profile

$$\eta(u) = \begin{cases} \eta_l, & u < \tilde{u}, \\ \eta_v, & u > \tilde{u} \end{cases} \quad (3.6)$$

as the initial approximation.

The characteristic initial parameter of the measuring scheme $\tilde{u}$ may be optimally selected by monitoring the behavior of the number of particles in a system in the course of the iteration process. At values of $\tilde{u}$ above some quantity u^* beginning with the specified time moment, the number of particles in a system increases consistently, thus corresponding to the stable convergence to a homogeneous liquid. When the values of $\tilde{u}$ are smaller than u^*, the number of particles in a system decreases beginning with the specified period of time, which corresponds to the stable convergence to a homogeneous vapor. The value of $\tilde{u}$ may always be selected so that it will be as close as possible to u^* within the limits of one step of the partition of the u-axis during the numerical solution of a problem.

During the numerical solution, in addition to parameter $\tilde{u}$, one more parameter L arises, which sets the upper boundary of the changes in variable u. At rather large values of L, it may be assumed that, in the $u > L$ range, the density reaches its bulk value. The selection of parameter L depends on the thickness of the transition layer, which varies with temperature. However, the value of L is not worth changing upon passing from one value of μ^* to another (at fixed values of temperature T and the number of partition intervals), because this may lead to jumps of nonphysical origin in the density profile behavior and relevant thermodynamic parameters.

To determine at which iteration we should terminate the iteration process, we observed, according to [1, 2], the behavior of grand thermodynamic potential Ω^* of a system. After several initial iterations during which the density profile is smoothed, the potential Ω^* virtually ceases to change. This means that we are in the vicinity of a critical nucleus. When the solution escapes this vicinity, Ω^* again begins to decrease abruptly. In order to select the most adequate approximation, we monitored the variation in the following parameters

$$\delta_1^{(k)} \equiv \frac{1}{n}\sum_{i=1}^{n} \left|\eta^{(k)}(u_i) - \eta^{(k-1)}(u_i)\right|, \quad (3.7)$$

$$\delta_2^{(k)} \equiv \frac{1}{n}\sum_{i=1}^{n} \left|\frac{\mu_h^*(\eta^{(k)}(u_i)) - \mu^* + \varphi(u_i)}{\mu_h^*(\eta^{(k)}(u_i))}\right|, \quad (3.8)$$

where n is the number of partition points, i is the number of a partition point, k is the iteration number, and $\varphi(u_i)$ is the integral in the left-hand side of equation (3.1). The values of $\delta_1^{(k)}$ and $\delta_2^{(k)}$ reach their minimal values at a point almost equal to k. The termination of the iteration process occurs precisely at these values of k.

We calculated profiles $\eta(u)$ for the Yukawa potential ($T_c = 0.0901\alpha/d^3 k_B$; α is the parameter of the Yukawa potential) at two temperatures T/T_c equal to 0.40 and 0.80, and for the Lennard-Jones potential ($T_c = 1.488\varepsilon/k_B$; ε is the parameter of the Lennard-Jones potential) at $T/T_c = 0.51$ and 0.80. Typical results are presented in Fig. 1. As is seen, at $T/T_c = 0.80$, the values of the density in the droplet center and in the vapor differ by a multiple of several tens, while the transition layer thickness appeared to be about $15d$. At $T/T_c = 0.40$ and 0.51, the densities differ already by a factor of 10^3 (which is typical, for example, of the nucleation in vapor under atmospheric conditions), whereas the transition layer thickness becomes about $5d$.

4. INHOMOGENEITY OF THE CENTRAL REGION OF SMALL DROPLET

When studying the density profiles obtained during the solution of equation (3.1), attention should be drawn to the fact that the density in the droplet center cannot be as high as the η_l corresponding to a homogeneous liquid. Moreover, there are virtually no homogeneous regions in the central parts of small droplets. One can only concede that a local homogeneity exists in the nucleus center in the proximity of point $u = 0$, where the

condition $(\partial\eta/\partial u)|_{u=0} = 0$ is always fulfilled. As the droplet grows, the volume of the homogeneous region increases, while the density in the droplet center approaches its value typical of the bulk liquid phase at the same value of chemical potential μ^*.

The inhomogeneity of the central region of a small droplet may be considered during homogeneous nucleation to be the result of self-overlapping of the surface layers of small nuclei, similar to the overlapping of the surface layers during heterogeneous nucleation [11]. In order to monitor the effect that this fact imposes on the behavior of various thermodynamic parameters, it is necessary to introduce a variable characterizing the nucleus size.

Let us take the radius R_e of an equimolar dividing surface as such a variable. This radius is defined by the condition

$$\int_V d\mathbf{r}\rho(r) = \frac{4\pi}{3}R_e^3\rho_l + \left(V - \frac{4\pi}{3}R_e^3\right)\rho_v, \qquad (4.1)$$

where ρ_v and ρ_l are the densities of bulk phases determined at chemical potential μ of a droplet. The following expression for dimensionless radius R_e^* of the equimolar dividing surface

$$R_e^{*3} = \frac{1}{\eta_v - \eta_l}\int_0^\infty du u^3 \frac{\partial\eta}{\partial u}(u) \qquad (4.2)$$

is evident from (4.1).

It is assumed that the number of particles inside the volume restrained by the equimolar dividing surface is nothing more than the number of particles ν in a nucleus. In the dimensionless variables, this number may be written as

$$\nu = 24\int_0^{R_e^*} du u^2\eta(u). \qquad (4.3)$$

Figure 2 represents the dependence of particle number density $\eta(0)$ in the droplet center on the radius R_e^* of the equimolar surface. Note that the curves obtained for the Yukawa and the Lennard-Jones potentials are similar. This implies that the Yukawa potential presents a qualitative true description of the behavior of small systems in terms of the density functional method.

Note the nonmonotonic pattern of the dependence of the central density on the droplet size. As large values of R_e^* become smaller, the value of $\eta(0)$ first rises, as is predicted by the classical theory with an allowance for the compressibility [12]. However, at yet smaller values of R_e^*, the density in the droplet center decreases abruptly and becomes smaller than the value corresponding to the bulk liquid phase, thus demonstrating the effect of self-overlapping of the surface

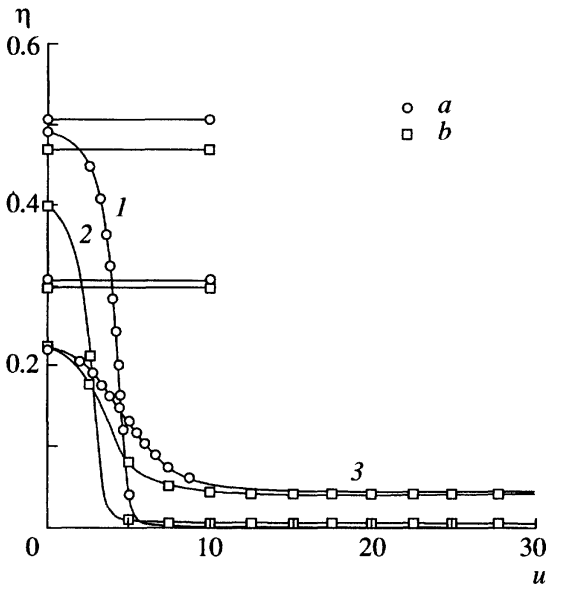

Fig. 1. Typical pattern of the density profiles $\eta(u)$ at T: (*1*) $0.40T_c$, (*2*) $0.51T_c$, and (*3*) $0.80T_c$. Horizontal lines indicate the values of the density of a homogeneous liquid at $\mu^* = \mu_\infty^*$. (*a*) The Yukawa potential, (*b*) the Lennard-Jones potential.

layer. As is seen from Fig. 2, the effect of self-overlapping is exhibited at the droplet sizes smaller than $10d$. Nonmonotonic behavior of the density in the droplet center as dependent on the droplet size is revealed also during gradient expansion in the density functional method [13]. A similar (in pattern) dependence of the density in the droplet center on the radius of the equimolar dividing surface was discovered also while modeling a droplet by the molecular dynamics method [14]. The last fact may confirm the applicability of the density functional method even for small droplets whose surface layer thickness is on the order of several interatomic distances.

The presence of the effect of self-overlapping makes it possible to state the existence of an analog of the disjoining pressure in small homogeneously nucleated droplets, which is usually observed in thin liquid films. All that has been said above may be illustrated by the dependences shown in Fig. 3. This figure represents the normal component of a pressure tensor in the droplet center calculated by the formula

$$p_N^*(0) = p_T^*(0) = p_h^*[\eta(0)] + \frac{1}{2}\eta(0)\int_V d\mathbf{u}' w^*(|\mathbf{u}'|)\eta(u') \qquad (4.4)$$

and the classical capillary approximation for the pressure in a droplet

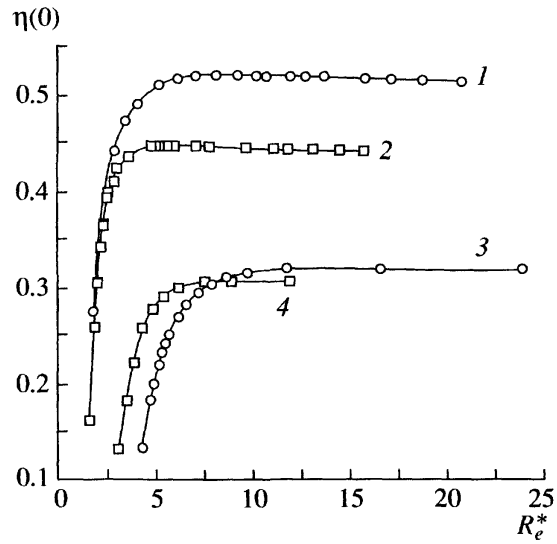

Fig. 2. Dependences of density η(0) in the droplet center on radius R_e^* of equimolar dividing surface at T: (*1*) $0.40T_c$, and (*3*) $0.80T_c$ for the Yukawa potential; (*2*) $0.51T_c$ and (*4*) $0.80T_c$ for the Lennard-Jones potential.

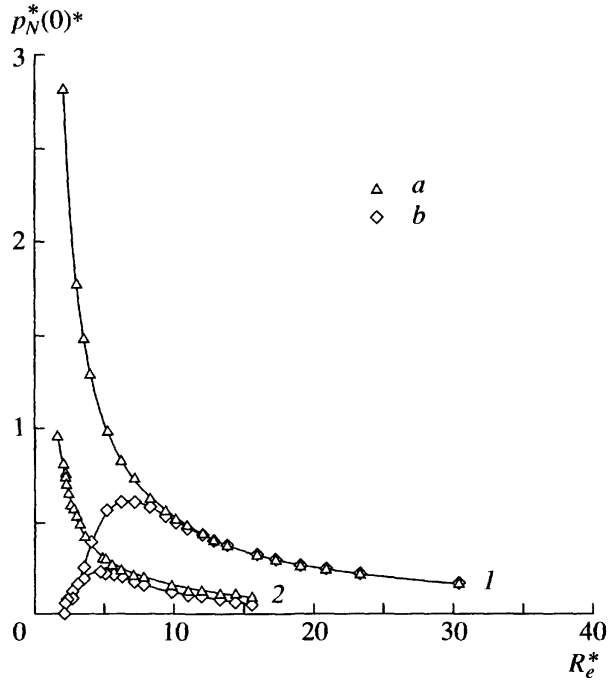

Fig. 3. Dependence of pressure p_N^* (0) in the droplet center on radius R_e^* of an equimolar dividing surface at T: (*1*) $0.40T_c$ for the Yukawa potential and (*2*) $0.51T_c$ for the Lennard-Jones potential; (*a*) capillary approximation; (*b*) normal component of pressure tensor in the droplet center.

$$p_{cap}^* = p_v^* + \frac{2\sigma_\infty^*}{R_e^*}, \qquad (4.5)$$

where the pressures of the liquid phase p_{cap}^* and vapor p_v^* are determined at the droplet chemical potential μ, and σ_∞^* is the dimensionless surface tension for the flat interface between the liquid and the vapor, which is related to the dimensional surface tension σ_∞ by the formula

$$\sigma_\infty^* = \pi d^2 \sigma_\infty / 6k_B T. \qquad (4.6)$$

To find σ_∞, we used the relationship following from the thermodynamic definition of the surface tension

$$\sigma_\infty = (\Omega_\infty + p_\infty V)/A_\infty, \qquad (4.7)$$

where A_∞ is the area of the interface and index ∞ indicates that all values were determined in the limit of the flat interface upon an equilibrium between the liquid and the vapor.

In the region of small R_e^*, a strong divergence of the curves (4.4) and (4.5) is observed; moreover, the behavior of the $p_N^*(0)$ function is nonmonotonic. Having in mind the definition of the disjoining pressure for a thin film, the pressure drop calculated by formulas (4.5) and (4.4) may be designated an analog of the disjoining pressure in small homogeneous droplets.

As is known [11], the disjoining pressure results in a nonmonotonic change in the chemical potential of the condensate in a droplet typical of the heterogeneous nucleation at wetting condensation nuclei. To analyze the effect of the inhomogeneity of the central region of homogeneously nucleated droplet on the chemical potential of its molecules, let us compare the dependences of the condensate chemical potential μ* on the number of molecules ν in a droplet. One of these dependences was obtained by the inversion of the ν(μ*) function obtained by the density functional method, while the other is presented by the classical capillary approximation

$$\mu_{cap}^* = \frac{2\sigma_\infty^*}{\eta_{l\infty} - \eta_{v\infty}} \left(\frac{8\eta_{l\infty}}{\nu}\right)^{1/3}. \qquad (4.8)$$

Let us recall that the values of the chemical potential in (4.8) are taken with reference to μ_∞^*; $\eta_{l\infty}$ and $\eta_{v\infty}$ are the densities of homogeneous liquid and vapor, respectively, at $\mu^* = \mu_\infty^*$. The results of calculations for dependences μ* and μ_{cap}^* are shown in Fig. 4 for two temperatures.

As is seen, in the region of small (on the order of several hundreds of particles) values of ν, the calculated curves for μ* and μ_{cap}^* diverge. Both curves ascend with decreasing ν; moreover, the rise in μ_{cap}^* is much steeper than that in μ*. However, this rise remains monotonic for both μ_{cap}^* and μ*.

Hence, the monotonic dependence of the condensate chemical potential is still the specific feature of the homogeneous mechanism of nucleation, even accounting for the inhomogeneity in the central region of a droplet. Consequently, an attempt at modifying the theory of homogeneous nucleation based on possible existence of a maximum on the curve of the condensate chemical potential in the region of small droplet sizes [15, 16] failed in the calculations performed by the density functional method.

The fact that the $\mu^*(\nu)$ curve passes below the $\mu^*_{cap}(\nu)$ curve indicates that the lowering of the activation barrier of nucleation resulted from the inhomogeneity in the droplet central region. Let us illustrate this barrier lowering by the dependence between the droplet formation work and droplet size. Let the vapor supersaturation be set by the value of chemical potential μ^*_v; then, the work of critical nucleus formation expressed in k_BT units has the form

$$W^*_c = \Omega^* + p^*_v V^*. \qquad (4.9)$$

To determine the dependence of the work of droplet formation on the number of particles in a droplet, let us use the general differential relationship $\partial W^*(\nu)/\partial\nu = \mu^*(\nu) - \mu^*_v$. Integrating this equation with respect to variable ν, we find that

$$W^*(\nu) = \int_{\nu_0}^{\nu}(\mu^*(\tilde{\nu}) - \mu^*_v)d\tilde{\nu} - \int_{\nu_0}^{\nu_c}(\mu^*(\tilde{\nu}) - \mu^*_v)d\tilde{\nu} + W^*_c, \qquad (4.10)$$

where ν_0 is a certain initial point on the $\mu^*(\nu)$ curve and ν_c is the size of the critical nucleus at $\mu^* = \mu^*_v$.

Let us consider now the $\mu^*(\nu)$ curve shown in Fig. 4. Let us take the minimal value of ν at this curve as ν_0. We compare the results obtained with the aid of (4.10) with the classical dependence $W^*_{cap}(\nu)$ obtained in the capillary approximation

$$W^*_{cap}(\nu) = \frac{6\sigma^*_\infty \eta^{1/3}_{l\infty}}{\eta_{l\infty} - \eta_{v\infty}}\nu^{2/3} - (\mu^*_v - \mu^*_\infty)\nu. \qquad (4.11)$$

The plots of dependences $W^*(\nu)$ and $W^*_{cap}(\nu)$ are presented in Fig. 5. As is seen, the maximum on the curve described by (4.10) lies below that on curve (4.11) (curves were plotted at a rather large value of μ^*_v, albeit corresponding to reasonable heights of the activation barrier of nucleation), thus precisely indicating that the nucleation barrier lowers.

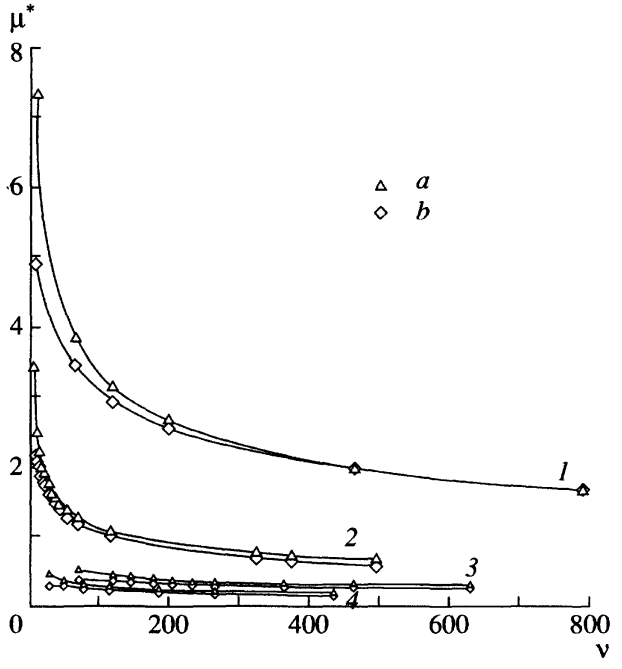

Fig. 4. Dependences of chemical potential μ^* on the number of molecules ν in a droplet at T: (*1*) $0.40T_c$ and (*3*) $0.80T_c$ for the Yukawa potential; (*2*) $0.51T_c$ and (*4*) $0.80T_c$ for the Lennard-Jones potential; (*a*) capillary approximation; (*b*) the density functional method.

Note that the inhomogeneity of the droplet central region affects also the dependence of the surface tension σ on the droplet size. This problem is being discussed in detail at present [5–7]; various authors employ different definitions of surface tension. We define σ_e for the equimolecular surface with radius R_e introduced by relationship (4.2) as

$$\sigma_e = \left[\frac{\Omega + p_v V}{4\pi R^2} + \frac{p_l - p_v}{3}R\right]\Bigg|_{R=R_e}, \qquad (4.12)$$

where p_l and p_v are the pressures in the liquid and gaseous bulk phases, respectively, at a given value of μ.

The dependence of surface tension σ^*_e for the equimolar dividing surface on its radius of curvature is shown in Fig. 6. As is seen, as R^*_e increases, the surface tension first rises rapidly, passes through a maximum, and then decreases slowly. Hence, σ^*_e varies in a nonmonotonic manner similarly to the behavior observed for the dependence of density and pressure in the droplet center on droplet size.

The value in square brackets in formula (4.12) is the general thermodynamic definition of the surface tension for an arbitrary spherical dividing surface of radius R. The application of this definition in the case $R = R_s$, where R_s is the radius of tension surface, determines the value of surface tension σ_s of the tension surface. As

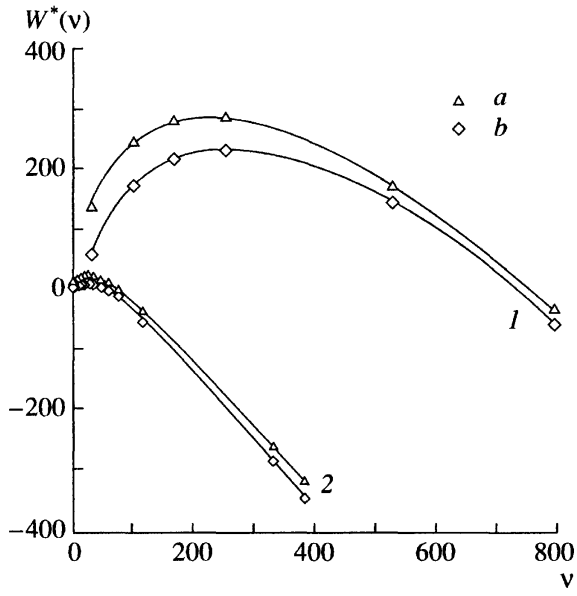

Fig. 5. Dependence of the droplet formation work $W^*(\nu)$ on the number of molecules ν in a droplet at T: (*1*) $0.40T_c$ for the Yukawa potential and (*2*) $0.51T_c$ for the Lennard-Jones potential. (*a*) Capillary approximation; (*b*) the density functional method.

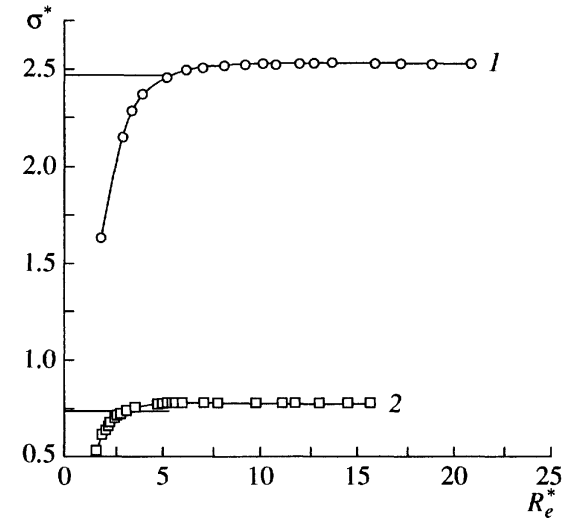

Fig. 6. Dependence of surface tension σ^* for an equimolecular dividing surface on its radius R_e^* at T: (*1*) $0.40T_c$ for the Yukawa potential and (*2*) $0.51T_c$ for the Lennard-Jones potential. Horizontal lines denote the values of σ_∞^*.

follows from (4.12), the values of σ_e and σ_s are interrelated by expression [17]

$$\sigma_e = \sigma_s\left[\frac{1}{3}\left(\frac{R_s}{R_e}\right)^2 + \frac{2}{3}\left(\frac{R_e}{R_s}\right)\right]. \qquad (4.13)$$

For large droplets, the dependence σ_s versus R_s is determined by the Tolman formula $\sigma_s = \sigma_\infty(1 - 2\delta_\infty/R_s)$ ($\delta_\infty = \lim_{R\to\infty}(R_e - R_s)$ is the Tolman length in the limit of a quasi-plane surface) with an accuracy of the terms of the first order with respect to small curvature. It follows from formula (4.13) that the differences between σ_e and σ_s are exhibited in the second order with respect to small parameter δ_∞/R_s; hence, for asymptotic $\sigma_e(R_e)$ in the quasi-plane approximation, we may write the expression

$$\sigma_e = \sigma_\infty(1 - 2\delta_\infty/R_e). \qquad (4.14)$$

As is seen from Fig. 6, the dependences $\sigma_e^*(R_e^*)$ reach their asymptotic value σ_∞^* as the upper limit for both potentials, although the deviations from σ_∞^* are small in the limit of large R_e^*. The Tolman length determined by the density functional method appeared to be a small (by its absolute value) negative value. The latter result was obtained earlier [5, 18] for the Lennard-Jones potential by the density functional method and from other considerations.

ACKNOWLEDGMENTS

This work was supported by the Russian Foundation for Basic Research, project no. 96-02-18959.

REFERENCES

1. Rowlinson, J. and Widom, B., *Molecular Theory of Capillarity*, Oxford (U.K.): Oxford Univ., 1978.
2. Oxtoby, D.W. and Evans, R., *J. Chem. Phys.*, 1988, vol. 89, no. 12, p. 7521.
3. Zeng, X.C. and Oxtoby, D.W., *J. Chem. Phys.*, 1991, vol. 94, no. 6, p. 4472.
4. Hadjiagapiou, I., *J. Phys.: Condens. Matter*, 1994, vol. 6, p. 5303.
5. Talanquer, V. and Oxtoby, D.W., *J. Phys. Chem.*, 1995, vol. 99, no. 9, p. 2865.
6. Laaksonen, A. and McGraw, R., *Europhys. Lett.*, 1996, vol. 35, no. 5, p. 367.
7. McGraw, R. and Laaksonen, A., *J. Chem. Phys.*, 1997, vol. 106, no. 12, p. 5284.
8. Evans, R., in *Fundamentals of Inhomogeneous Fluids*, Henderson, D., Ed., Wiley, 1992.
9. Carnahan, N.F. and Starling, K.E., *J. Chem. Phys.*, 1969, vol. 51, no. 1, p. 635.
10. Weeks, J.D., Chandler, D., and Andersen, H.C., *J. Chem. Phys.*, 1996, vol. 54, no. 12, p. 5237.
11. Kuni, F.M., Shchekin, A.K., Rusanov, A.I., and Widom, B., *Adv. Colloid Interface Sci.*, 1996, vol. 65, p. 71.

12. Kuni, F.M., Shchekin, A.K., and Rusanov, A.I., *Kolloidn. Zh.*, 1993, vol. 45, no. 4, p. 682.

13. Falls, A.N., Scriven, L.E., and Davis, H.T., *J. Chem. Phys.*, 1981, vol. 75, no. 8, p. 3986.

14. Thompson, S.M., Gubbins, K.E., Walton, J.P.R.B., Chantry, R.A.R., and Rowlinson, J.S., *J. Chem. Phys.*, 1984, vol. 81, no. 1, p. 530.

15. Rasmussen, D.H., *J. Cryst. Growth*, 1982, vol. 56, no. 1, p. 45.

16. Hale, B.N., *Phys. Rev., A: Gen. Phys.*, 1986, vol. 33, no. 6, p. 4156.

17. Ono, S. and Kondo, S., *Molecular Theory of Surface Tension in Liquids*, Springer: Berlin, 1960.

18. van Giessen, A.E., Blokhuis, E.M., and Bukman, D.J., *J. Chem. Phys.*, 1998, vol. 108, p. 1148.